

## Aligned Arrays of Fe<sup>3+</sup> Ions Decorated TiO<sub>2</sub> Nanotubes for Photocatalytic Application under Sunlight Irradiation

WEIMING WU

College of mechanical and Electronic Engineering, Chuzhou University, Chuzhou 239000, Anhui Province, P.R. China

Corresponding author: Tel: +86 15955011545; E-mail: wwm97@163.com

Received: 13 November 2013;

Accepted: 13 March 2014;

Published online: 26 December 2014;

AJC-16504

Titanium dioxide nanotubes arrays were successfully synthesized by an anodizing route, which were designed as a photocatalyst. Through adsorbing Fe<sup>3+</sup> ions on the surface of the TiO<sub>2</sub> nanotubes, their photocatalytic activity can be effectively improved. The photodegradation experiments show that, under presence of H<sub>2</sub>O<sub>2</sub>, the methylene blue pollutant (1 × 10<sup>-6</sup> M) was almost completely decomposed by as-fabricated Fe<sup>3+</sup> ions doped TiO<sub>2</sub> nanotubes arrays under irradiation of sunlight for 0.5 h. Comparing with the pure TiO<sub>2</sub> nanotubes arrays photocatalysts, the photocatalytic activity of the Fe<sup>3+</sup> ions doped TiO<sub>2</sub> nanotubes arrays is obviously higher.

**Keywords:** TiO<sub>2</sub> nanotube, Fe<sup>3+</sup> ions, Decorating, Sunlight irradiation.

### INTRODUCTION

With the development of industrialization, the environment is suffering serious damage. The purification of environment is a problem that needs to be resolved on priority basis. Titanium dioxide (TiO<sub>2</sub>), as a key material for photocatalytic oxidation, provides a unique opportunity for the purification of environment. Under illumination of UV-light, TiO<sub>2</sub> photocatalyst can be successfully used to purify water and air, to degrade the organic pollutants and to kill the bacteria<sup>1-3</sup>. However, for all practical applications, it is more desirable that TiO<sub>2</sub> photocatalyst can be applied under visible light or sunlight irradiation. Unfortunately, the pure TiO<sub>2</sub> photocatalyst itself does not allow the use of visible light. Therefore, a number of studies have been focused on preparation of more efficient visible light and sunlight photocatalyst<sup>4-7</sup>. One approach has been to dope transition metals into TiO<sub>2</sub><sup>8-10</sup> and another has been to form reduced TiO<sub>x</sub> photocatalysts<sup>11,12</sup>. However, doped materials suffer from a thermal instability<sup>9</sup> and increase of carrier recombination centers, or the requirement of an expensive ion implantation facility<sup>10</sup>. Due to these subsistent problems, those achievements are not enough compared to the performance demanded by the practical application.

According to the photocatalytic mechanism of TiO<sub>2</sub>, the photon energy excites electrons (e<sup>-</sup>) from valence band (VB) to the conduction band (CB) of the TiO<sub>2</sub>, leaving holes (h<sup>+</sup>) in the valence band. Then, these photon-generated electrons and holes are able to initiate redox reactions with chemical species adsorbed on the surface or interface of photocatalyst as soon

as they can be transferred to the surface of TiO<sub>2</sub>. Thus the photocatalytic activity is mainly controlled by the rate of reduction and oxidation by e<sup>-</sup> and h<sup>+</sup> and the rate of e<sup>-</sup>/h<sup>+</sup> recombination. The potential of e<sup>-</sup> and h<sup>+</sup> are constant unless the crystal structure of the photocatalyst is changed. However, the amount of substrate adsorbed depends more directly on the nature of the surface, *e.g.* specific surface area. Herein, we designed the Fe<sup>3+</sup> ions doped TiO<sub>2</sub> nanotubes (Fe-TN) arrays photocatalytic system that possesses highly efficient photocatalytic activity under sunlight irradiation. The aligned tubular TiO<sub>2</sub> arrays with high specific surface area, which could improve the rate of e<sup>-</sup> and h<sup>+</sup> transfer across the surface of the semiconductor. And the doping of Fe<sup>3+</sup> ions on their surface can inhibit photon-generated electrons and holes recombination to improve effectively the photocatalytic activity. We suggest that it is of significantly importance for practical applications of TiO<sub>2</sub> in photocatalytic filed.

### EXPERIMENTAL

Firstly, the TiO<sub>2</sub> nanotubes arrays were fabricated by anodizing the pure Ti sheet as described previously<sup>13,14</sup>. In brief, high-purity (99.999 %) titanium plate was cleaned in acetone. Then the substrate were rinsed with deionized water and dried in vacuum. Electrochemical anodization was carried out in a two-electrode cell and graphite served as a counter electrode. The titanium plate was anodized in mixing electrolyte of ethylene glycol and hydrofluoric acid (0.2 M) for 10 h. The anodizing voltage was 100 V and the temperature of the

electrolyte was kept constant at 15 °C. After the electrochemical anodization the samples was rinsed with deionized water and dried in vacuum. Subsequently, the as-fabricated TiO<sub>2</sub> nanotubes arrays were annealed at 450 °C for 3 h. Finally, the annealed TiO<sub>2</sub> nanotubes arrays were immersed into dilute FeCl<sub>3</sub> aqueous solution for 1 h to obtain Fe<sup>3+</sup> ions doped TiO<sub>2</sub> nanotubes arrays, then dried in vacuum at 70 °C.

The photocatalytic activities of the Fe<sup>3+</sup> doped TiO<sub>2</sub> nanotubes arrays were evaluated by the removal of methylene blue (MB) dye in aqueous solution. Before experiment, an adsorption/desorption equilibrium of methylene blue on the surfaces of these TiO<sub>2</sub> nanotubes arrays was established *via* immersing these samples into the methylene blue aqueous solution in dark for 20 min. And the concentration of the solution was determined, which was considered as initial concentration ( $C_0$ ) of the methylene blue dye. The changes of the concentration of methylene blue were monitored by a UV-visible spectroscopy at scheduled irradiation time. The photocatalysis experiments were performed under sunlight irradiation. In order to improve the recurrence of Fe<sup>2+</sup> to Fe<sup>3+</sup> ions, the dilute H<sub>2</sub>O<sub>2</sub> aqueous solution (10 mM) was added to the methylene blue aqueous solution.

## RESULTS AND DISCUSSION

Fig. 1 shows top-view and cross-sectional SEM images of the as-prepared TiO<sub>2</sub> nanotubes (TN) array morphology. It can be observed that highly ordered TN arrays were composed of nanotubes with inner diameter of 100 nm and wall thickness of 25 nm, respectively. The inset in Fig. 1a shows the bottom view of TN arrays, it is apparent that the tubes are closed with a TiO<sub>2</sub> layer on the bottom. And the tubes formed under the electrochemical condition (Fig 1b) are entirely smooth. The visible-Raman spectra of pure TN sample employing the 514.5 nm laser as the excitation source is presented in Fig. 2. The pure TN shows major Raman bands of TiO<sub>2</sub> anatase at 141, 393, 513 and 637 cm<sup>-1</sup>, which can be attributed to the Raman-active modes of anatase phase with the symmetries of E<sub>g</sub>, B<sub>1g</sub>, A<sub>1g</sub> and E<sub>g</sub>, respectively<sup>15</sup>.

Fig. 3 shows the UV-visible absorption spectra of initial methylene blue (1 × 10<sup>-6</sup> M) and methylene blue after being degraded under sunlight irradiation for 0.5 h. To ensure the same experimental condition, all the amount of used methylene

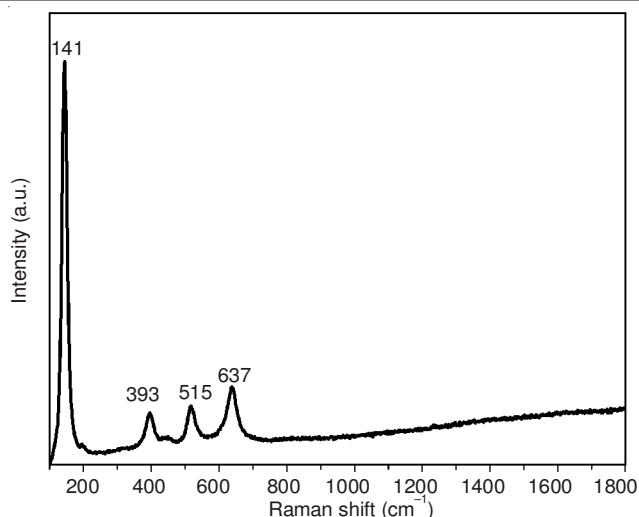


Fig. 2. Visible-Raman spectra of TN arrays annealed at 450 Celsius-degree

blue aqueous solution was 10 mL to which was added 10 mM H<sub>2</sub>O<sub>2</sub> and the experiments were performed at the same time to keep the same intensity of sunlight. Before being degraded (curve a), the absorption peak at about 660 nm for the initial methylene blue aqueous solution is very strong. After degradation, it is observed that the photocatalytic degradation of methylene blue self-fading (curve b) is lower than that of TiO<sub>2</sub> nanotubes and Fe<sup>3+</sup> doped TiO<sub>2</sub> nanotubes arrays photocatalysts. Moreover, the photodegradation activity of the Fe<sup>3+</sup> doped TiO<sub>2</sub> nanotubes arrays (curve d) is higher than that of the pure TiO<sub>2</sub> nanotubes arrays (curve c). The methylene blue pollutant was almost completely decomposed under irradiation of sunlight after 0.5 h. In order to markedly compare the photocatalytic activity of the Fe<sup>3+</sup> doped TiO<sub>2</sub> nanotubes and the pure TiO<sub>2</sub> nanotubes arrays, the concentration of methylene blue dye aqueous solution were increased to 5 × 10<sup>-5</sup> M, the concentration of H<sub>2</sub>O<sub>2</sub> is still 10 mM. Fig. 4 shows the kinetic curves of photocatalytic degradation of methylene blue (5 × 10<sup>-5</sup> M) on the different photocatalytic systems. The methylene blue concentration removal rate may be expressed as C/C<sub>0</sub>, where C<sub>0</sub> and C are the initial and real time concentration of methylene blue aqueous solution during the reaction, respectively. It is clearly demonstrated that the Fe<sup>3+</sup> doped TiO<sub>2</sub> nanotubes arrays achieved the best performance for methylene

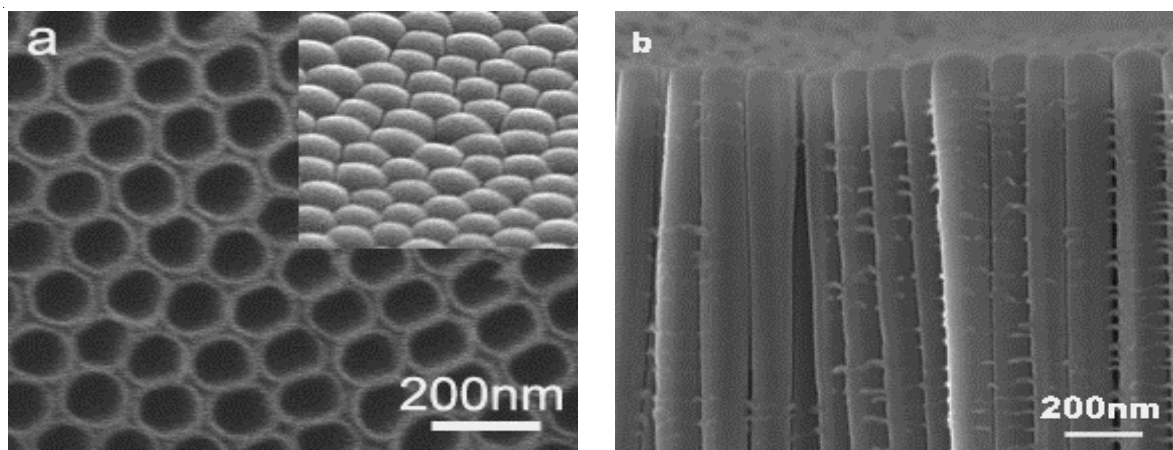


Fig. 1. SEM images of the TN arrays: (a) top surface, the inset for the bottom surface; (b) cross section

blue photodegradation. The degradation course of Fe<sup>3+</sup> doped TiO<sub>2</sub> nanotubes arrays photocatalyst to methylene blue is different from that of pure TiO<sub>2</sub> photocatalyst. As for the pure TiO<sub>2</sub> photocatalyst, the photon-generated electrons (e<sup>-</sup>) and holes (h<sup>+</sup>) react with HO<sup>-</sup> and O<sub>2</sub> to produce the hydroxyl radical (OH) which are able to degrade methylene blue. However, in the Fe<sup>3+</sup> doped TiO<sub>2</sub> nanotubes arrays photocatalyst, the Fe<sup>3+</sup> ions on the surface of TiO<sub>2</sub> nanotubes, as strong oxidizable ions, initiate redox reactions with methylene blue and transform into Fe<sup>2+</sup> ions. The Fe<sup>2+</sup> ions are relatively unstable as compared to Fe<sup>3+</sup> ions, which have half-filled *d* orbitals (*d*<sup>5</sup>). Therefore, there is a tendency for the transformation from Fe<sup>2+</sup> ions to Fe<sup>3+</sup> ions. Under the H<sub>2</sub>O<sub>2</sub> condition, the Fe<sup>2+</sup> ions are returned to Fe<sup>3+</sup> ions again (eqn. 2). Finally, an electron of OH<sup>-</sup> is extracted to transfer into hydroxyl radical (OH) by photon-generated holes of TiO<sub>2</sub> (eqn. 4). These reactions form a circulation as following:

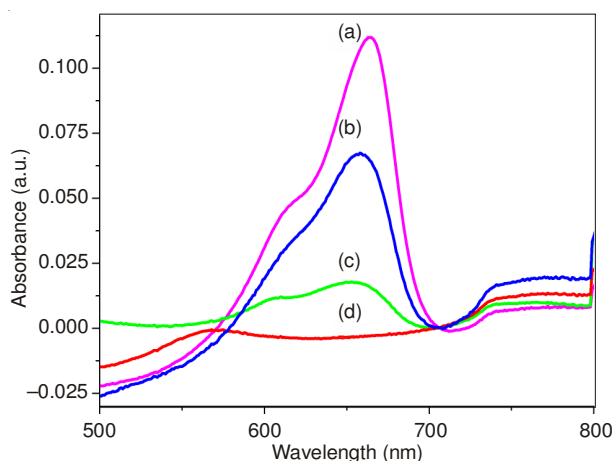
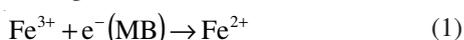


Fig. 3. UV-visible absorption spectra of initial methylene blue (MB) ( $1 \times 10^{-6}$  M) with 10 nm H<sub>2</sub>O<sub>2</sub> (a) and after being degraded by (b) self-photofading; (c) TN arrays; (d) Fe-TN arrays under sunlight irradiation for 0.5 h

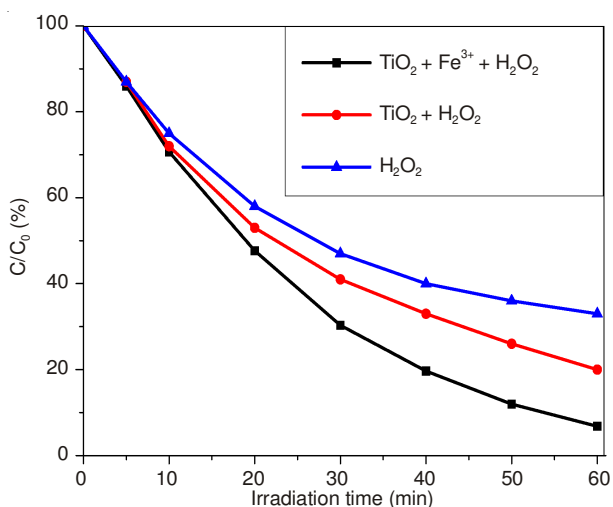
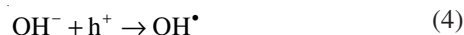
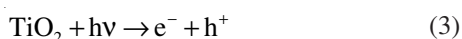
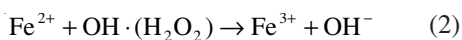
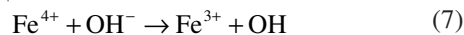


Fig. 4. Kinetic curves of photocatalytic of methylene blue (MB) on the different photocatalysts under presence of H<sub>2</sub>O<sub>2</sub>



All these take advantage for improving the photocatalytic activity of the system to increase the degrading efficiency of system to methylene blue. At beginning of photogradation, the difference among the degradation rate of methylene blue with the assistance of the three systems is not very distinct. This reason is that the H<sub>2</sub>O<sub>2</sub> [ $E^0(\text{H}_2\text{O}_2/\text{H}_2\text{O}) = 1.77$  V] in the methylene blue aqueous solution, initiates redox reactions with methylene blue, which is more prominent than the degradation of Fe<sup>3+</sup> ions and TiO<sub>2</sub> nanotubes arrays photocatalysts to methylene blue at the initial stages. 20 min later, the concentration of H<sub>2</sub>O<sub>2</sub> decreases, the oxidibility of the aqueous solution is attenuated, which results in the lowering of the degradation rate. However, for the Fe<sup>3+</sup> doped TiO<sub>2</sub> nanotubes arrays photocatalyst, the Fe<sup>3+</sup> ions still initiate redox reactions with methylene blue to transform into Fe<sup>2+</sup> ions, then the oxidizability of the remanent H<sub>2</sub>O<sub>2</sub> is enough to re-oxidate the Fe<sup>2+</sup> ions to Fe<sup>3+</sup> ions ( $E^0(\text{Fe}^{3+}/\text{Fe}^{2+}) = 0.77$  V). Meanwhile, the photon-generated holes transfer from TiO<sub>2</sub> nanotube to bound OH<sup>-</sup> and produce hydroxyl radical. Therefore, the recurrent reactions as the equations of (1-4) shown can be ceaselessly occurred, which improve the utilization rate of photon-generated electrons and holes of TiO<sub>2</sub>. Thus the degradation rate of methylene blue is kept at a fast and hardly variational speed after 20 min.

In absence of the H<sub>2</sub>O<sub>2</sub>, the Fe<sup>3+</sup> ions act as both a photo-generated hole and an electron trap and inhibit the hole-electron recombination as follows (5-6). And the unstable Fe<sup>4+</sup> and Fe<sup>2+</sup> ions on the surface of TiO<sub>2</sub> nanotubes arrays will initiate the reactions (7-8) to release the hole and electron.



Therefore, the doping of Fe<sup>3+</sup> ions can ensure the transfer of the photon-generated electrons and holes to the surface of TiO<sub>2</sub> nanotube to improve the photocatalytic activity of the system. The kinetic curves of photocatalytic degradation of methylene blue ( $5 \times 10^{-5}$  M) on the different photocatalytic systems in absence of the H<sub>2</sub>O<sub>2</sub> was shown in Fig. 5. The experiments were also preformed under unlight irradiation and the used methylene blue is not added the H<sub>2</sub>O<sub>2</sub>. It is apparent that the photocatalytic activity of Fe<sup>3+</sup> doped TiO<sub>2</sub> nanotubes arrays is still higher than that of the pure TiO<sub>2</sub> nanotubes arrays and methylene blue self-photo-fading<sup>16</sup>. Moreover, the photocatalytic activity of Fe<sup>3+</sup> doped TiO<sub>2</sub> nanotubes arrays under without the H<sub>2</sub>O<sub>2</sub> is lower than the one under with it.

## Conclusion

We designed the tubular nanostructured TiO<sub>2</sub> aligned arrays as photocatalysts. In order to improve the photocatalytic activity, the Fe<sup>3+</sup> ions were used to decorate the TiO<sub>2</sub> nanotubes aligned arrays. The as-fabricated Fe<sup>3+</sup> doped TiO<sub>2</sub> nanotubes arrays possess higher photocatalytic activity. Under irradiation of sunlight for 0.5 h, the methylene blue ( $1 \times 10^{-6}$  M) pollutant with the H<sub>2</sub>O<sub>2</sub> was almost completely decomposed. And

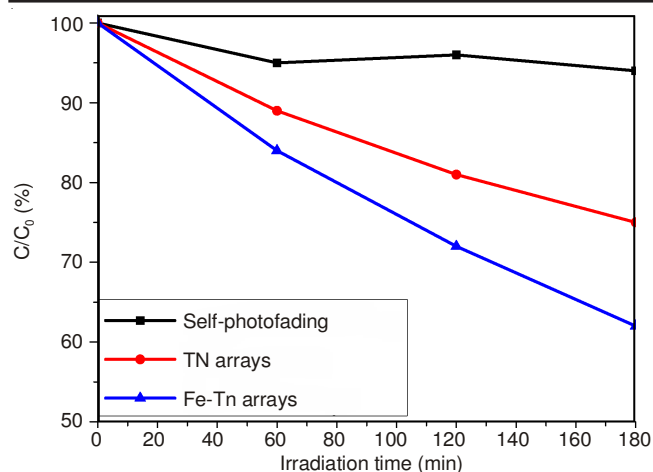


Fig. 5. Kinetic curves of photocatalytic of methylene blue (MB) on the different photocatalysts under absence of  $H_2O_2$

comparing with the pure  $TiO_2$  nanotubes arrays photocatalysts, the photodegradation rate of the  $Fe^{3+}$  doped  $TiO_2$  nanotubes arrays for methylene blue is obviously higher. It is found that the photocatalytic activity of  $Fe^{3+}$  doped  $TiO_2$  nanotubes arrays in the methylene blue aqueous solution without the  $H_2O_2$  is lower than that of with the  $H_2O_2$ , but it still achieves the best performance for methylene blue among the pure  $TiO_2$  nanotubes arrays and methylene blue self-photofading under absence of  $H_2O_2$ . Furthermore, we suggested that the high photocatalytic activity of  $Fe^{3+}$  doped  $TiO_2$  nanotubes arrays is ascribed to the decoration of  $Fe^{3+}$  ions which changed the course of photodegradation of  $TiO_2$  to methylene blue and improved the utilization rate of photon-generated electrons and holes of  $TiO_2$ .

## ACKNOWLEDGEMENTS

This research was supported by National Major Project of Fundamental Research: Nanomaterials and Nanostructures (Grant No. 2005CB623603) and the National Natural Science Foundations of China (Grant No. 90406008 and 10674138).

## REFERENCES

1. M.R. Hoffmann, S.T. Martin, W.Y. Choi and D.W. Bahnemann, *Chem. Rev.*, **95**, 69 (1995).
2. L.X. Cao, A.M. Huang, F.J. Spiess and S.L. Suib, *J. Catal.*, **188**, 48 (1999).
3. S. Sato, T. Kadowaki and K. Yamaguti, *J. Phys. Chem.*, **88**, 2930 (1984).
4. S. Sakthivel and H. Kisch, *Angew. Chem. Int. Ed.*, **42**, 4908 (2003).
5. I. Tsuji, H. Kato, H. Kobayashi and A. Kudo, *J. Am. Chem. Soc.*, **126**, 13406 (2004).
6. X. Wang, S. Meng, X. Zhang, H. Wang, W. Zhong and Q. Du, *Chem. Phys. Lett.*, **444**, 292 (2007).
7. Y. Li, D.-S. Hwang, N.H. Lee and D.-J. Kim, *Chem. Phys. Lett.*, **404**, 25 (2005).
8. D.W. Hess, *J. Electrochem. Soc.*, **124**, 735 (1977).
9. W. Choi, A. Termin and M.R. Hoffmann, *J. Phys. Chem.*, **98**, 13669 (1994).
10. M. Anpo, *Catal. Surv. Jpn.*, **1**, 169 (1997).
11. R. Breckenridge and W. Hosler, *Phys. Rev.*, **91**, 793 (1953).
12. D.C. Cronemeyer and W.R. Hosler, *Phys. Rev.*, **113**, 1222 (1959).
13. S.P. Albu, A. Ghicov, J.M. Macak, R. Hahn and P. Schmuki, *Nano Lett.*, **7**, 1286 (2007).
14. J.M. Macak, H. Tsuchiya, L. Taveira, S. Aldabergerova and P. Schmuki, *Angew. Chem. Int. Ed.*, **44**, 7463 (2005).
15. T. Ohsaka, F. Izumi and Y.J. Fujiki, *Raman Spectrosc.*, **7**, 321 (1978).
16. S. Jain, G. Dangi, J. Vardia and S.C. Ameta, *Int. J. Energy Res.*, **23**, 71 (1999).